

# SUBSURFACE STRUCTURE OF BATURAGUNG ESCARPMENT REVEALED THROUGH THREE- DIMENSIONAL GRAVITY INVERSION

## *STRUKTUR BAWAH PERMUKAAN PEGUNUNGAN BATURAGUNG DITINJAU MENGGUNAKAN INVERSI 3D ANOMALI GRAVITASI*

Selvi Misnia Irawati<sup>1\*</sup>, Alutsyah Luthfian<sup>2</sup>, Agus Laesanpura<sup>3</sup>

<sup>1</sup>Geophysical Engineering, Institut Teknologi Sumatera

<sup>2</sup>School of Environment, Auckland University

<sup>3</sup>Geophysical Engineering, Institut Teknologi Bandung

Received: 2021, January 7<sup>th</sup>

Accepted: 2021, March 5<sup>th</sup>

Keyword:

Baturagung Escarpment;

Gravity;

Inverse modeling;

SimPEG.

Correspondent Email:

[selvi.irawati@tg.itera.ac.id](mailto:selvi.irawati@tg.itera.ac.id)

How to cite this article:

Irawati, S.M., Luthfian, A., &  
Laesanpura, A. (2021).

Subsurface Structure of  
Baturagung Escarpment

Abstract. Baturagung Escarpment is an essential tectonic element of Java Island because it represents a transition from the Southern Mountain Block to the Kendeng Basin. This study has succeeded in producing a three-dimensional model of the Baturagung Escarpment subsurface using gravity anomaly data. The data are distributed along a regional scale transect, whose resolving capability has been tested using a checkerboard test. Our proposed geophysical model can fit the observed data very well, with a 0.77% RMS error. This model exhibits a structural depression bounded by high basement blocks below the Baturagung Escarpment, one of the basement block outcrops at Jiwo Hills. The maximum width of the depression is ~10 km, with a depth exceeding 3 km in some places. The depression might be formed because of an extensional tectonic regime that prevailed during the Palaeogene, followed by volcanic arc loads' emplacement up to the early Miocene.

*Abstrak. Pegunungan Baturagung adalah salah satu unsur tektonik penting di Pulau Jawa karena mewakili transisi dari Blok Pegunungan Selatan ke Cekungan Kendeng. Dalam penelitian ini, kami berhasil membuat suatu model geofisika tiga dimensi bawah permukaan Pegunungan Baturagung dengan menggunakan metode gravitasi. Data gravitasi yang kami gunakan dikumpulkan pada titik-titik yang tersebar pada lintasan pengukuran skala regional. Uji papan catur telah memastikan bahwa persebaran titik-titik kami mampu mencapai target penelitian, yaitu keberadaan struktur geologi di bawah Pegunungan Baturagung. Model geofisika yang kami usulkan dapat memberikan nilai*

Revealed Through Three Dimensional Gravity Inversion. *Jurnal Geofisika Eksplorasi*, 07(01), 17-29.

© 2021 JGE (Jurnal Geofisika Eksplorasi). This article is an open access article distributed under the terms and conditions of the Creative Commons Attribution (CC BY NC)

*anomali yang sesuai dengan data pengamatan (ralat RMS sebesar 0.77%). Model tersebut menunjukkan keberadaan cekungan yang berjurus Timur Laut – Barat Daya dengan lebar maksimal ~10 km di bawah Pegunungan Baturagung. Kedalaman maksimum dari cekungan ini > 3 km. Cekungan ini dibatasi oleh blok batuan dasar yang salah satu bagiannya tersingkap di Perbukitan Jiwo. Kami menginterpretasikan bahwa cekungan tersebut bisa terbentuk karena adanya tektonik ekstensi selama masa Paleogen diikuti dengan pembebanan dari busur vulkanik hingga Miosen awal.*

## 1. INTRODUCTION

In the study of the tectonics of Java Island, the Baturagung Escarpment is of utmost importance because it represents the transition from the Southern Mountain Block to the Kendeng Basin (Smyth et al., 2008). Baturagung Escarpment is composed of Cenozoic sedimentary strata that sit unconformably above a Mesozoic metamorphic basement (Figure 1) that crops out as Jiwo Hills (Rahardjo et al., 1995; Smyth et al., 2008; Surono et al., 1992).

Several theories have been proposed for the formation of Baturagung Escarpments, such as thrusting of Southern Mountain Block (Hall et al., 2007), vertical block faulting (Rahardjo et al., 1995; Surono et al., 1992), or northward-dipping normal fault (Bemmelen, 1949). However, such theories were developed upon surficial geological examinations, which may deviate from the actual subsurface conditions. Inspection of subsurface geology requires interpretation of geophysical data using an objective mathematical technique, such as inverse modeling (Milsom & Eriksen, 2011).

In this study, we will investigate the subsurface features of the Baturagung Escarpment by constrained inversion of gravity anomaly data. The inversion strategy applied here will follow that of Miller et al. (2017), supplemented with applying a reference model to guide the inversion process.

## 2. PREVIOUS STUDIES

Regional-scale gravity anomaly mapping around the Baturagung Escarpment has been conducted by Sato and Untung (1978), Budiman (1991), Marzuki and Otong (1991), and Haryono et al. (1995). More recent gravity anomaly studies in the region have been targeting local-scale anomalies, e.g., Arief et al. (2009) and Sihombing et al. (2015). However, all those studies were modeling the anomaly using 2D or 2.5D source bodies.

In this study, we will model the gravity anomaly data using 3D volume elements (voxel). The theoretical background of 3D gravity modeling has been explained in detail by Li and Oldenburg (1998). Three-dimensional gravity modeling has been applied in Indonesia, e.g., to resolve magmatic intrusion below Gunung Pandan (Wahyudi et al., 2019), hydrocarbon-producing anticline in Borneo (Christensen et al., 2018), and subsurface structures related to Sidoarjo Mudflow (Osorio et al., 2019).

## 3. METHODS

We use gravity anomaly data gathered over Baturagung Escarpment by an exploration group of Institut Teknologi Bandung (Figure 1). The gravity data is then reviewed and processed into complete Bouguer anomaly using formulas presented in Hinze et al. (2005) and Hinze et al. (2013). The complete Bouguer

anomaly is devoid of gravity effect from an ideal terrain above a vertical datum (Hinze et al., 2005). To calculate the effect of ideal terrain above the vertical datum (WGS84 ellipsoid) we build a MATLAB routine using Eq. 32 of Rousset et al. (2015). The value of rock density used for the data processing is 2.67 g/cm<sup>3</sup>. Because we are interested in the local-scale

subsurface geology, we use the residual Bouguer anomaly to produce the density model. Calculation of the residual Bouguer anomaly  $A_R(x,y)$  follows this formula (Hinze et al., 2013).

$$A_R(x,y) = A(x,y) - A_R(x,y) \quad (1)$$

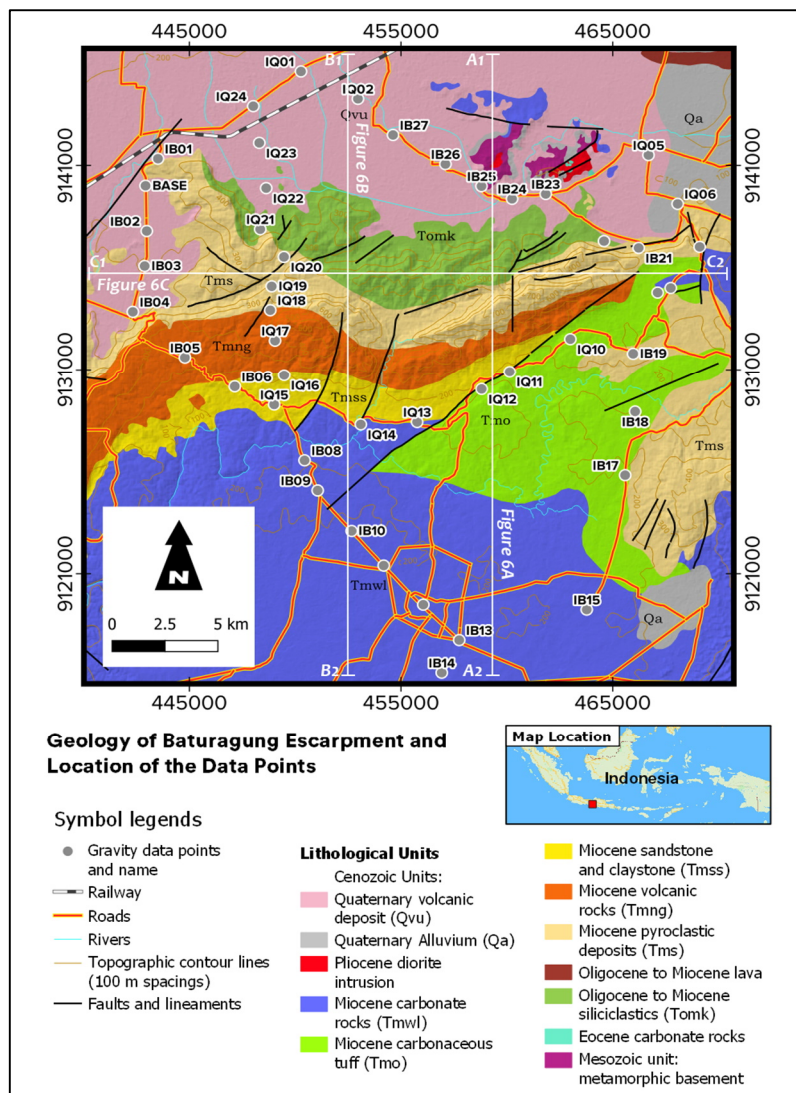


Figure 1. Geologic map of Baturagung Escarpment along with the location of gravity data points (grey dots, some unnumbered). Geologic data is compiled from Rahardjo et al. (1995) and Surono et al. (1992). Contour lines, rivers, road lines, and railway tracks are extracted from 1:250,000 national topographic map (Bakosurtanal, 2003). Location of profiles shown in Figure 6 is given as straight white lines with remarks.

In the eq. (1),  $A(x,y)$  denotes the complete Bouguer anomaly, and  $A_R(x,y)$  symbolizes the

regional Bouguer anomaly. To compute the regional Bouguer anomaly, this study uses a

simple planar surface approximation of the form  $A_R(x, y) = A + Bx + Cy$  (Draper & Smith, 1981). The simple planar surface approximation is chosen to replicate the regional gravity effect given by the southwestern edge of the Merapi-Lawu Anomaly (Luehr et al., 2013).

To model the gravity data, we use the SimPEG package (Cockett et al., 2015). To run the modeling process, SimPEG can use raw point data as its input, and no prior gridding is required (Cockett et al., 2015; Miller et al., 2017). Thus, SimPEG is suitable for modeling gravity data collected at unevenly spaced points on topographically challenging regions (Miller et al., 2017).

The modeling process of SimPEG sought to minimize the objective function  $\phi(m)$  (Cockett et al., 2015).

$$\phi(m) = \phi_d(m) + \beta\phi_m(m) \quad (2)$$

An array of proposed model values is denoted by  $m$ . On the right-hand side of Eq. (2),  $\beta$  is a positive constant referred to as trade-off parameter, regression parameter, regularization parameter, or Tikhonov parameter (Tikhonov et al., 1995). Misfit between the observation data and modeled values is denoted by  $\phi_d(m)$ .

$$\phi_d(m) = \mathbb{E} \cdot \|W_d(F[m] - d_{obs})\|_2^2 \quad (3)$$

In Eq. (3) above,  $W_d$  is a diagonal matrix whose diagonal elements are equal with  $1/\epsilon_i$ , where  $\epsilon_i$  equals to the estimated value of the standard deviation of the  $i$ th data. The modeled gravity values are symbolized by  $F[m]$ , with  $F[\dots]$  acts as an operator that calculates the gravity effect from the model  $m$ . Observed gravity data is denoted by  $d_{obs}$  (Cockett et al., 2015; Miller et al., 2017).

On the other hand,  $\phi_m(m)$  is calculated using the following equation.

$$\phi_m(m) = \mathbb{E} \cdot \|W_m(m - m_{ref})\|_2^2 \quad (4)$$

Eq. (4) above represents a measure of misfit between current model  $m$  and a priority model  $m_{ref}$ . This study uses a two-layered finite rectangular block model for  $m_{ref}$ , with an upper layer density of  $2.3 \text{ g/cm}^3$  and a lower layer density of  $3 \text{ g/cm}^3$ .

The difference between  $m$  and  $m_{ref}$  is weighted by  $W_m$ , a matrix whose elements are defined by eq. (5) below.

$$W_m = [\alpha_s I, \alpha_x W_x^T, \alpha_y W_y^T, \alpha_z W_z^T]^T \quad (5)$$

Both  $\alpha_*$  and  $W_*$  controls the smoothness of the density model. Smaller values of  $\alpha_*$  and  $W_*$  (minimum zero) will lead to a blocky density model, suitable in areas with sharp density contrasts (Cockett et al., 2015; UBC-GIF, 2015a). In this study, we use these values for  $W_m$ .

$$W_m = [2, 2, 2, 2]^T \quad (6)$$

Using  $W_m$  value described in eq. (6) will guarantee that the inversion process produces a model that is midway between smooth and blocky (UBC-GIF, 2015b). Our study also limits the inversion process to fill the density model with values ranging from  $2.3$  to  $3 \text{ g/cm}^3$ . The lower search limit would indicate the bulk density of cavernous limestone, while the upper one would denote the bulk density of metamorphic and igneous basement (Jacoby & Smilde, 2009).

## 4. RESULTS AND DISCUSSION

### 4.1. Sensitivity Test

To demonstrate that our data point distribution is sufficient for resolving the subsurface structures below the Baturagung Escarpment, we did a sensitivity test. In the test, we simulate a gravity anomaly measurement over a checkerboard density model below the Baturagung Escarpment topographic surface. The location of measurement is equal to the position of our data points, and the gravity anomaly values at

that point are treated as the observation data. We then model the subsurface density using the observed gravity anomaly data, with parameters and reference model described in section (3). The results of our sensitivity test are presented in Figures 2 and 3.

SimPEG inversion procedure successfully recovers the gravity anomaly produced by the checkerboard pattern measured on our data point. The amplitude of difference between the observed checkerboard anomaly (Figure 2A) and the calculated anomaly (Figure 2B) is no more than 0.03 mGal (Figure 2C). The RMS error of the calculated anomaly is 0.01 mGal. In producing the three-dimensional density model, the inversion ran for 35 iterations and converged after 30 iterations (Figure 2D).

The three-dimensional density models calculated from the checkerboard gravity effect observed at our data points have patterns that matched the original checkerboard (Figure 3). However, the original density values are not recovered well (Figure 3B and 3D). In the calculated model, deeper voxels have a lesser density difference between the initially negative and positive checkerboard density blocks. Another striking feature of the calculated density model (Figure 3B and 3D) is the presence of fictitious circular high-density voxels surrounding data points located in the initially negative density checkerboard blocks.

#### **4.2. Baturagung Escarpment Gravity Anomaly**

Figure 4 shows the residual gravity anomaly as measured over Baturagung Escarpment. A zone of gravity low is evident at the northeastern, central, western, and southern parts of the survey area (Figure 4A). The inversion process converges after 20 iterations (Figure 4D) and successfully reconstructed the observed anomaly (Figure 4B) with RMS error 0.77 mGal (0.77% of data amplitude). The differences between the

calculated and observed anomaly are mostly within 2 mGal (Figure 4C). The large differences at the northwestern data points may hint at the insufficient data sampling over a concealed geologically complex region.

Modeling of residual gravity anomaly data shows the presence of NW–SE trending, ~10 km-wide depression below the Baturagung Escarpment (Baturagung Depression, Figure 5). The depression is bounded by fault associated with Baturagung Escarpment (Figure 5B). High-density basement block that outcrops at the northern part of the survey area (Figure 1), bounds the northern limit of the sedimentary basin (Figure 5 and 6). Block faulting that bounds the northern limit of the Baturagung Depression (Figure 6A and 6B) closely supports the geological cross-section proposed by Surono et al. (1992). In the deepest part of the Baturagung Depression, the contact between the low-density sediments and the basement might occur at a depth of more than 3 km (Figure 6). Bodies of relatively higher density embedded in the sedimentary layer (Figure 5A and 6) may reflect the presence of buried remnants of igneous masses related to the Late Oligocene – Early Miocene volcanoes around the Baturagung Depression (Hartono & Bronto, 2007; Smyth et al., 2011).

In our model, the basement block that limits the southern side of Baturagung Depression extends far beyond our survey area (Figure 5 and 6). The northern basement block, however, is restricted by a fault that cuts the northern part of our survey area (Figure 5 and 6B). The fault, which trends from E to W, might have played an essential role in the tilting of Baturagung Escarpment and compressional tectonic features observed (Husein et al., 2008; Purnomo & Purwoko, 1994).

#### **4.3. Formation of Baturagung Depression**

The presence of a geological depression beneath the Baturagung Escarpment is a novel

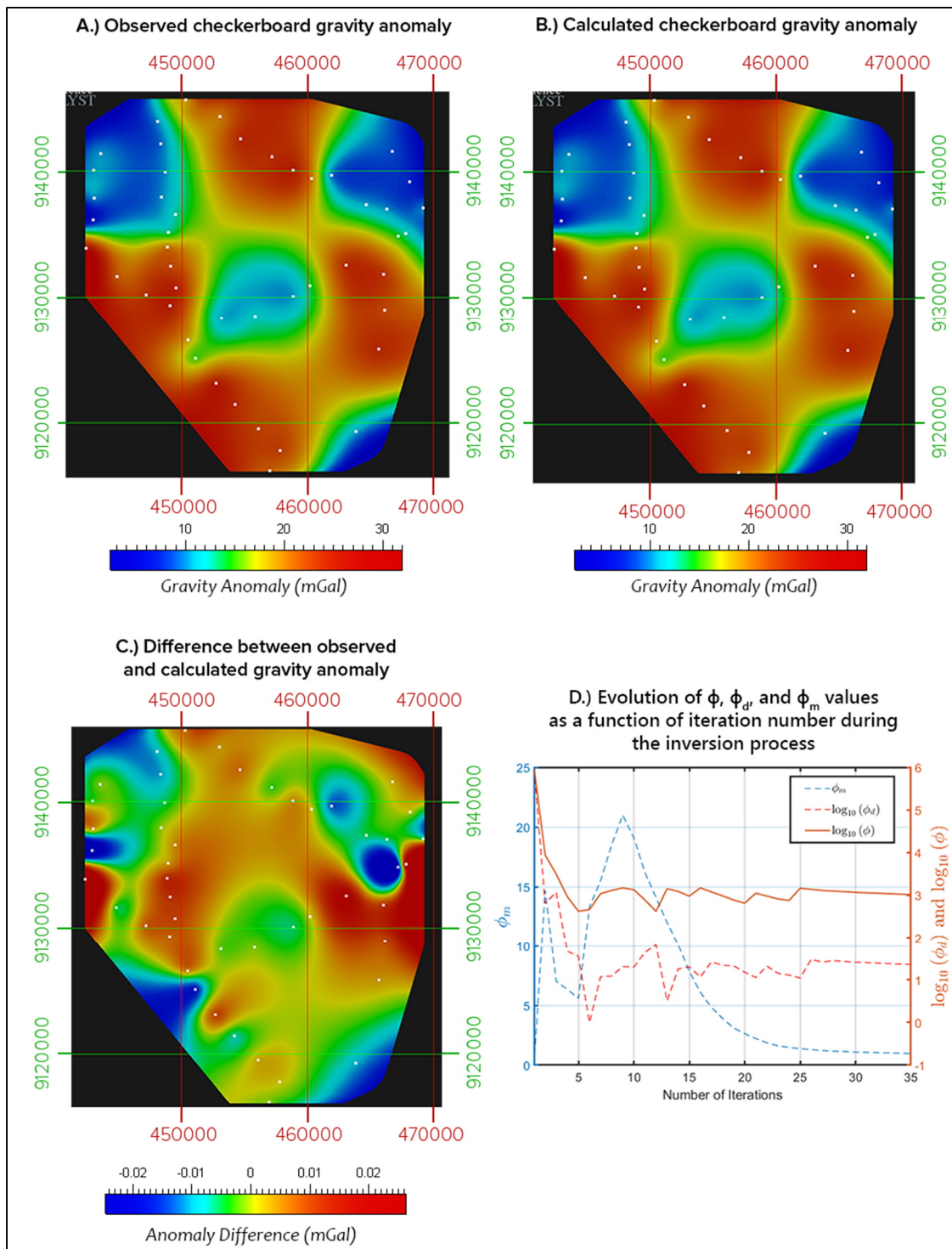


Figure 2. Observed (A) and calculated (B) gravity anomaly from the checkerboard sensitivity test. The difference between the observed and calculated gravity anomaly is given in (C). Figure (D) describes the evolution of  $\phi$ ,  $\phi_d$ , and  $\phi_m$  as a function of the model evolved by the  $i - th$  iteration (Eq. 2). Colours in (A) to (C) describes gravity anomaly values in mGals, with the respective colour scale below each figure. Figure (A) to (C) are plotted on UTM 49S grid coordinate system, and locations of the gravity anomaly data points are marked with white dots. The values of  $\phi$ ,  $\phi_d$ , and  $\phi_m$  in (D) are unitless.

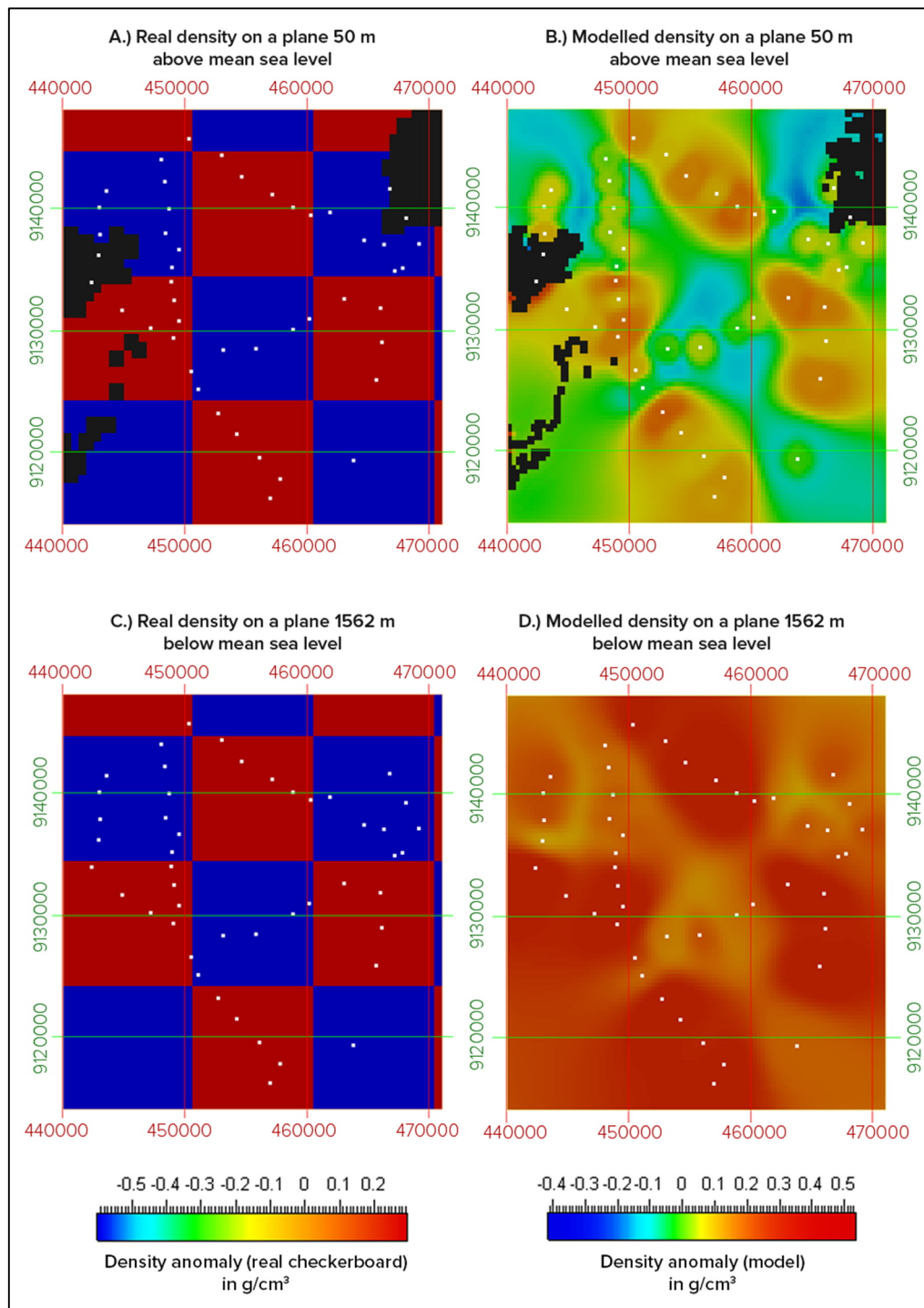


Figure 3. Inverse modelling results from the checkerboard gravity anomaly values. Figure (A) and (C) respectively show the original checkerboard pattern on a plane 150 metres (A) and 1200 metres (C) below the Baturagung Escarpment surface. The colour scale for the original checkerboard pattern (Figure A and C) is shown below figure (C). Figure (B) and (D) shows the density model recovered from checkerboard gravity anomaly “observed” at our data points; density model is sliced at 150 metres (B) and 1200 metres (D) below the Baturagung Escarpment surface. Colour scale for Figure (B) and (D) is indicated below (D). The colour fillings of the figures denote density values in  $\text{g/cm}^3$ , and all data shown here are plotted over UTM 49S grid coordinate system.

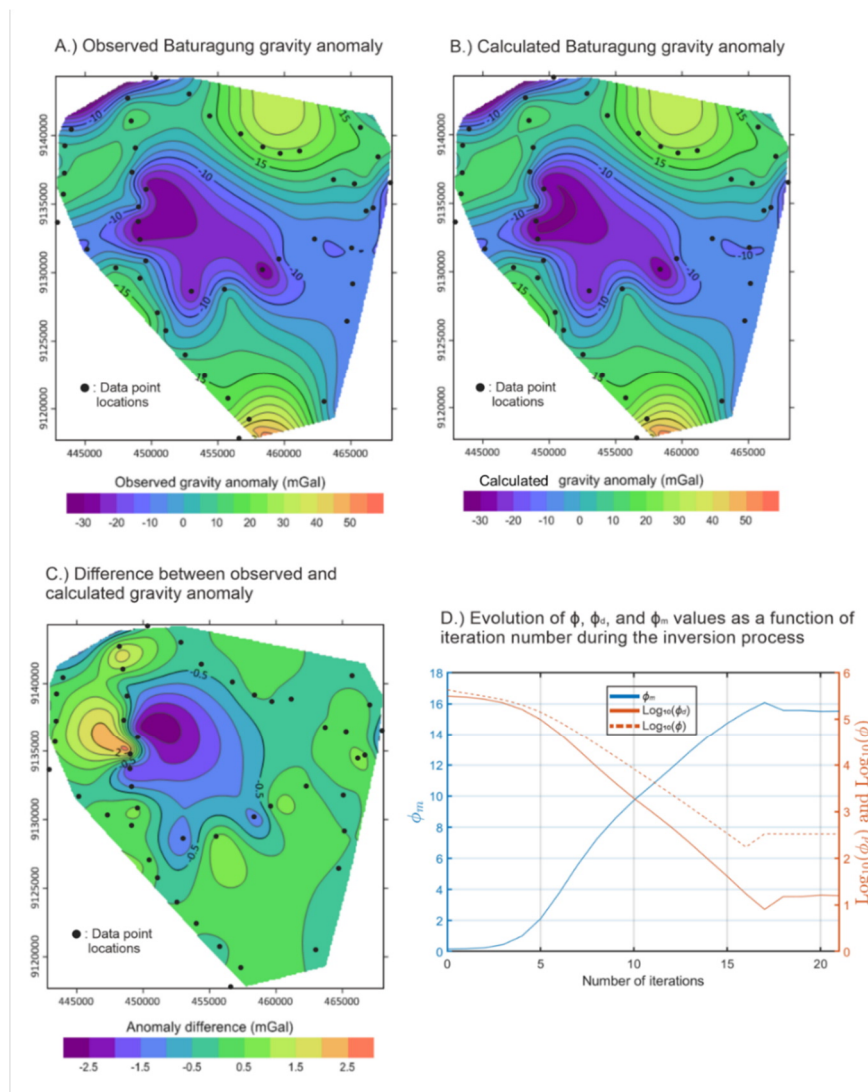


Figure 4. Observed (A) and calculated (B) gravity anomaly from the Baturagung Escarpment gravity anomaly. The difference between the observed and calculated gravity anomaly is given in (C). Figure (D) describes the evolution of  $\phi$ ,  $\phi_d$ , and  $\phi_m$  as a function of the model evolved by the  $i - th$  iteration (Eq. 2). Colours in (A) to (C) describes gravity anomaly values in mGals, with the respective colour scale below each figure. Figure (A) to (C) are plotted on UTM 49S grid coordinate system, and locations of the gravity anomaly data points are marked with white dots. The values of  $\phi$ ,  $\phi_d$ , and  $\phi_m$  in (D) are unitless.

idea for most geologists dealing with the tectonics of the Javanese Southern Mountains. Nevertheless, the presence of such feature in the Southern Mountains region has been postulated by Julias et al. (2017). The

alignment of the Baturagung Depression is perpendicular to the Meratus Trend (Figure 7) that hosts several grabens that opened during the Paleogene (Mulyawan & Husein, 2014; Purnomo & Purwoko, 1994).

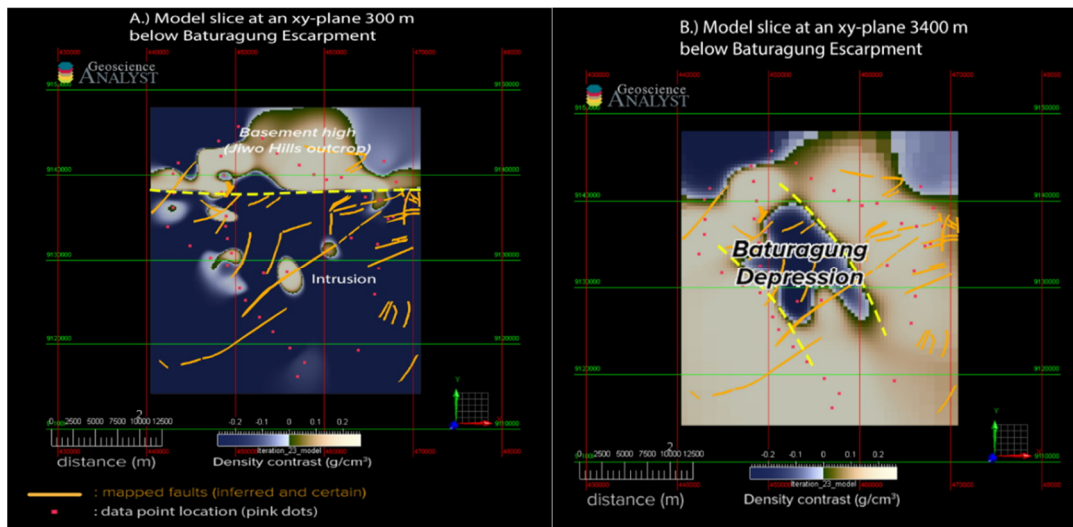


Figure 5. Slices of the three-dimensional density model produced by inverting the residual gravity anomaly data presented in Figure 4. The value of density contrast (departure from the ideal  $2.67 \text{ g/cm}^3$ ) is expressed as colour variation indicated below each figure. In (A), we present the model slice on a plane located 300 metres below the Baturagung Escarpment surface, while in (B) we present the model slice on a plane located 3400 meters below the Baturagung Escarpment surface. The location of Baturagung Depression is indicated in figure (B), and all identifiable structures in the model is marked by dashed yellow lines. All figures are plotted over UTM 49S grid coordinate system.

The grabens are directed from NW to SE as a response to the SSE-NNW directed compressive stresses (Purnomo & Purwoko, 1994; Gultaf, 2014). The deepening process of the Baturagung Depression may continue well into the early Miocene ( $\sim 20 \text{ Ma}$ ) due to the loads from the Southern Mountains Volcanic Arc mass.

## 5. CONCLUSION AND FUTURE WORKS

We have successfully produced a new subsurface density model of the Baturagung Escarpment using gravity anomaly data. The data were collected at distributed points that can objectively resolve large-scale regional geological structures in the region. Modeling of the residual gravity anomaly revealed the presence of a concealed geological depression beneath the Baturagung Escarpment, which we called as Baturagung Depression. Near the surface, the depression is at maximum  $\sim 10 \text{ km}$  wide, and it gets narrower with depth. In the deepest part of the depression, the thickness of the sedimentary layer exceeds  $3 \text{ km}$ .

Baturagung Depression might be formed because of a prevailing extensional tectonic regime during the Paleogene ( $30\text{-}40 \text{ Ma}$ ) followed by the emplacement of volcanic arc loads up to the early Miocene ( $\sim 20 \text{ Ma}$ ).

Future works in the Baturagung Escarpment should be directed into refining our subsurface model by incorporating the available or acquiring new gravity data. It is also possible to improve our model using the available borehole and geological dataset from various sources. A better understanding of Baturagung Escarpment geology will improve our knowledge of the tectonic processes that have affected Java Island, especially during the Cenozoic.

## ACKNOWLEDGEMENTS

The writer would be grateful for the help and assistance offered by various parties during the course of fieldwork, data processing, analysis, and paper writing. The first author would like to thank ITERA for supporting this research.

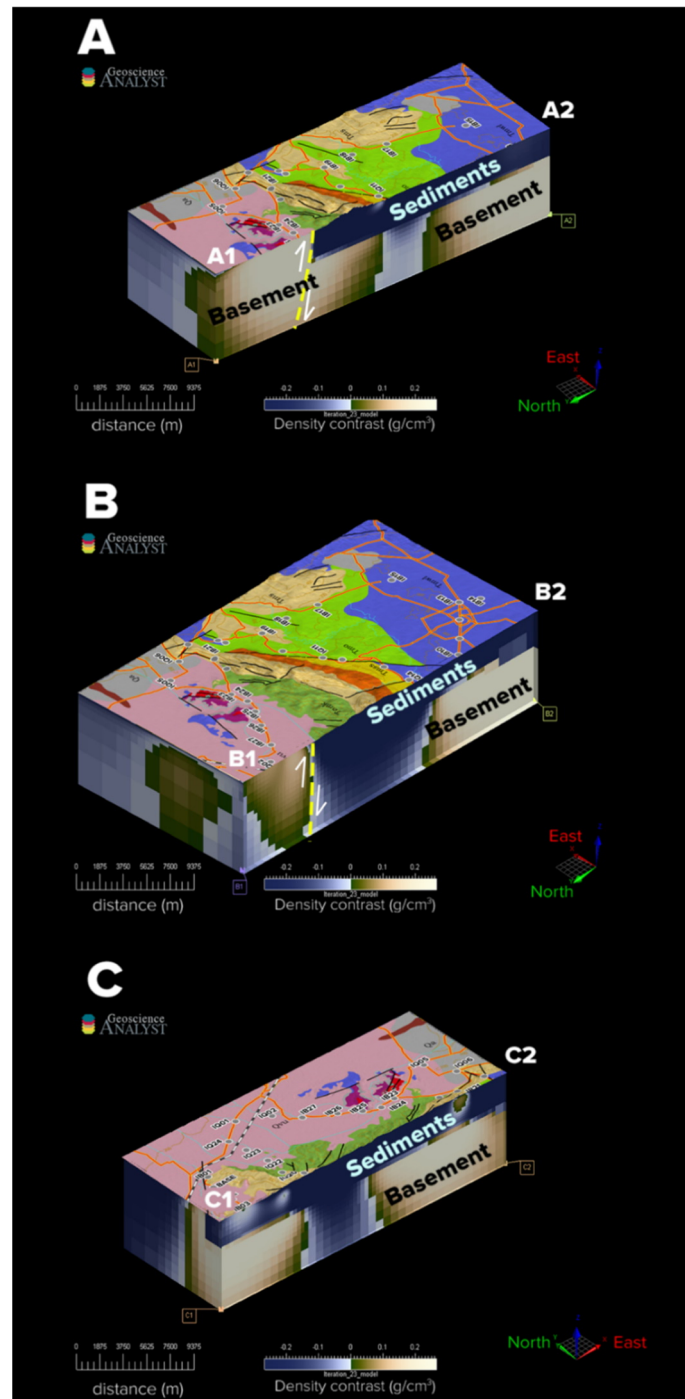


Figure 6. Vertical slices of the three-dimensional density model produced by inverting the residual gravity anomaly data presented on Figure 4. The location of respective slices (A, B, C) is presented in Figure 1. The values of density anomaly (departure from the ideal rock density of 2.67 g/cm<sup>3</sup>) is presented as colour variation indicated below each figure. Structures identifiable in the model is marked by dashed yellow line. Geologic map from Figure 1 is draped over the topographic surface cover of the density model.

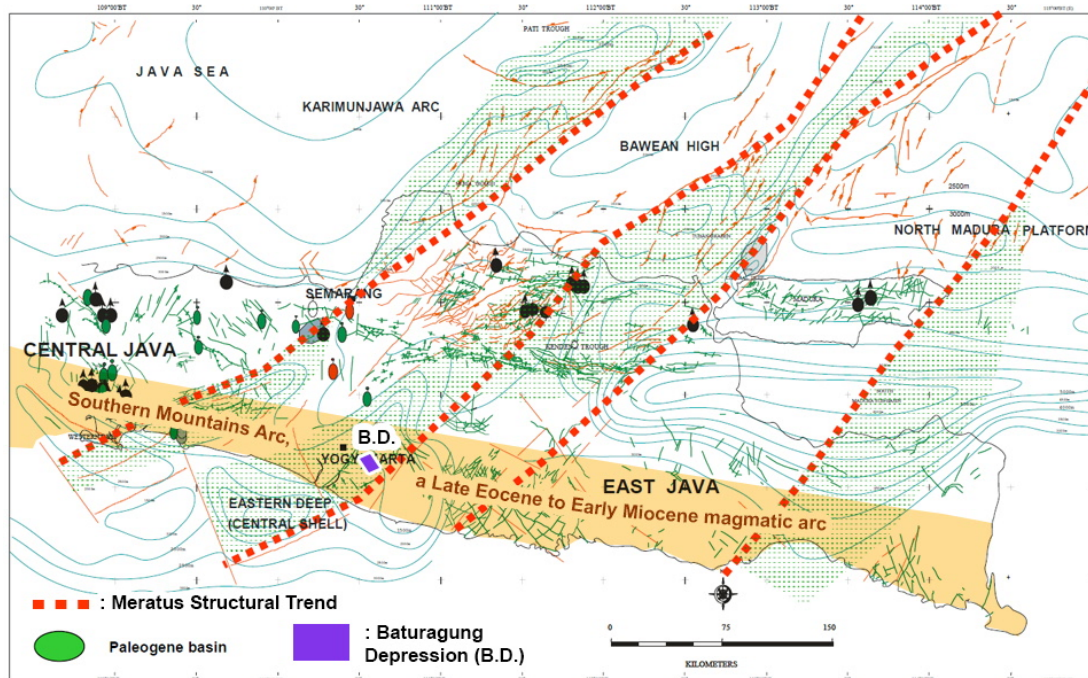


Figure 7. The position of Baturagung Depression in the Eastern Java tectonic framework. Baturagung Depression is a part of Paleogene structures that is perpendicular to the Meratus Trend (Subroto et al., 2007). The deepening of Baturagung Depression might continue well up to the Early Miocene due to volcanic arc loading (Waltham et al., 2008) from the Southern Mountain magmatism (Smyth et al., 2008; Soeria-Atmadja et al., 1994).

## REFERENCES

- Arief, D., Nurdien, I., Darmawan, H., Sudrajat, I., Hartono, R., Afif, H., Rasyid, A., Niasari, S. W., Wahyudi, & Suyanto, I. (2009). Pemetaan Bawah Permukaan Intrusi Diorit Menggunakan Metode Gravitasi, Magnetik dan AMT di Jiwo Barat, Bayat, Klaten, Jawa Tengah. International Conference on Earth Science and Technology, Yogyakarta, Indonesia.
- Bakosurtanal. (2003). *Lembar 1408 Yogyakarta* [Topographic Map]. Cibinong, Indonesia, Badan Informasi Geospasial. <https://tanahair.indonesia.go.id/portal-web/downloadpetacetak?skala=250K>
- Bemmelen, R. W. V. (1949). *The geology of Indonesia* (Vol. IA). Government Printing Office.
- Budiman, I. (1991). *Interpretation of gravity data over central Jawa, Indonesia* [Masters Thesis, University of Adelaide]. Adelaide, Australia. <https://digital.library.adelaide.edu.au/dspace/handle/2440/110285>
- Christensen, A. N., Jones, C., Kocijan, L. B., Booth, H., Rouxel, S., & Kunjan, B. (2018). Airborne Gravity Gradiometer Survey over the Pelarang Anticline, Onshore Kutai Basin, Indonesia. *ASEG Extended Abstracts, 2018(1)*, 1-6. [https://doi.org/10.1071/ASEG2018ABT7\\_3B](https://doi.org/10.1071/ASEG2018ABT7_3B)
- Cockett, R., Kang, S., Heagy, L. J., Pidlisecky, A., & Oldenburg, D. W. (2015). SimPEG: An Open Source Framework For Simulation And Gradient Based Parameter Estimation In Geophysical Applications. *Computers & Geosciences, 85*, 142-154. <https://doi.org/https://doi.org/10.1016/j.cageo.2015.09.015>
- Draper, N. R., & Smith, H. (1981). *Applied Regression Analysis* (2nd edition ed.). John Wiley & Sons, Inc.
- Gultaf, H. (2014). *Analisa Kinematik Sesar Grindulu di Daerah Pacitan dan Sekitarnya* [Master's thesis, Bandung Institute of

- Technology]. Bandung, Indonesia. <https://digilib.itb.ac.id/index.php/gdl/view/41622>
- Hall, R., Clements, B., Smyth, H. R., & Cottam, M. A. (2007). A New Interpretation of Java's Structure. *Indonesian Petroleum Association Proceedings 31st Annual Convention and Exhibition*, Jakarta, Indonesia.
- Hartono, G., & Bronto, S. (2007). Asal-usul Pembentukan Gunung Batur di daerah Wediombo, Gunungkidul, Yogyakarta. *Indonesian Journal on Geoscience*, Vol 2, No 3, 2007. <http://ijog.bgl.esdm.go.id/index.php/IJOG/article/view/35>
- Haryono, S., Otong, R., & Oyon, S. (1995). *Peta anomali Bouguer lembar Surakarta & Giritontro, Jawa*. Bandung, Indonesia, Direktorat Geologi.
- Hinze, W. J., Aiken, C., Brozena, J., Coakley, B., Dater, D., Flanagan, G., Forsberg, R., Hildenbrand, T., Keller, G. R., Kellogg, J., Kucks, R., Li, X., Mainville, A., Morin, R., Pilkington, M., Plouff, D., Ravat, D., Roman, D., Urrutia-Fucugauchi, J., Véronneau, M., Webring, M., & Winester, D. (2005). New standards for reducing gravity data: The North American gravity database. *GEOPHYSICS*, 70(4), J25-J32. <https://doi.org/10.1190/1.1988183>
- Hinze, W. J., Frese, R. R. B. V., & Saad, A. H. (2013). *Gravity and Magnetic Exploration: Principles, Practices, and Applications*. Cambridge University Press. <https://doi.org/DOI:10.1017/CBO9780511843129>
- Husein, S., Mustofa, A., Sudarno, I., & Toha, B. (2008). Tegalrejo Thrust Fault as an Indication of Compressive Tectonics in Baturagung Range, Bayat, Central Java. *Pertemuan Ilmiah Tahunan Ikatan Ahli Geologi Indonesia ke-37*, Bandung, Indonesia.
- Jacoby, W., & Smilde, P. L. (2009). *Gravity Interpretation: Fundamentals and Application of Gravity Inversion and Geological Interpretation* (1st ed.). Springer-Verlag Berlin Heidelberg. <https://doi.org/10.1007/978-3-540-85329-9>
- Julias, R. N., Muslih, Y. B., Agatra, G., Nugraha, A., Ramadhan, T., & Husein, S. (2017, September 25 – 28 ). Surface Evidences on Understanding Paleogene Structure between Kendeng Basin with East Java Basin and Southern Mountain. *Joint Convention Malang 2017*, Malang, Indonesia.
- Li, Y., & Oldenburg, D. W. (1998). 3-D inversion of gravity data. *GEOPHYSICS*, 63(1), 109-119. <https://doi.org/10.1190/1.1444302>
- Luehr, B.-G., Koulakov, I., Rabbel, W., Zschau, J., Ratdomopurbo, A., Brotopuspito, K. S., Fauzi, P., & Sahara, D. P. (2013). Fluid Ascent and Magma Storage Beneath Gunung Merapi Revealed by Multi-Scale Seismic Imaging. *Journal of Volcanology and Geothermal Research*, 261, 7-19. <https://doi.org/https://doi.org/10.1016/j.jvolgeores.2013.03.015>
- Marzuki & Otong, R. (1991). *Peta Anomali Bouguer Lembar Yogyakarta, Jawa*. Bandung, Direktorat Geologi.
- Miller, C. A., Williams-Jones, G., Fournier, D., & Witter, J. (2017). 3D Gravity Inversion And Thermodynamic Modelling Reveal Properties Of Shallow Silicic Magma Reservoir Beneath Laguna del Maule, Chile. *Earth and Planetary Science Letters*, 459, 14-27. <https://doi.org/https://doi.org/10.1016/j.epsl.2016.11.007>
- Millsom, J., & Eriksen, A. (2011). *Field Geophysics* [English] (4th ed.). John Wiley & Sons, Inc.
- Mulyawan, R. S., & Husein, S. (2014). Kompleks Sesar Trembono Sebagai Gravitational Structures. *Seminar Nasional Kebumihan ke-7*, Yogyakarta, Indonesia.
- Osorio, Á., Mauri, G., Mazzini, A., & Miller, S. (2019). Geological 3D Model of The Lusi Mud Edifice Based on Gravity Data, East Java, Indonesia [Article]. *Geophysical Research Abstracts*, 21, 1-1. <https://ezproxy.auckland.ac.nz/login?url=http://search.ebscohost.com/login.aspx?direct=true&db=aph&AN=140485261&site=ehost-live&scope=site>
- Purnomo, J., & Purwoko. (1994). Kerangka Tektonik dan Stratigrafi Pulau Jawa Secara Regional dan Kaitannya dengan Potensi

- Hidrokarbon. Seminar Jurusan Teknik Geologi, Yogyakarta, Indonesia.
- Rahardjo, W., Sukandarrumidi, & Rosidi, H. M. D. (1995). *Peta Geologi Lembar Yogyakarta, Jawa*. Bandung, Pusat Penelitian dan Pengembangan Geologi.
- Roussel, C., Verdun, J., Cali, J., & Masson, F. (2015). Complete Gravity Field of An Ellipsoidal Prism by Gauss–Legendre Quadrature. *Geophysical Journal International*, 203(3), 2220-2236. <https://doi.org/10.1093/gji/ggv438>
- Sato, Y., & Untung, M. (1978). *Gravity and Geological Studies in Jawa, Indonesia*. Geological Survey of Indonesia.
- Sihombing, D. P., Destawan, R., Ady, S., & Fajri, Z. R. (2015). Geological Subsurface Investigation by Using the Integration of Gravity and Magnetic Methods at Bayat, Central Java, Indonesia. In *Near-Surface Asia Pacific Conference, Waikoloa, Hawaii, 7-10 July 2015* (pp. 418-421). Society of Exploration Geophysicists, Australian Society of Exploration Geophysicists, Chinese Geophysical Society, Korean Society of Earth and Exploration Geophysicists, and Society of Exploration Geophysicists of Japan. <https://doi.org/10.1190/nsapc2015-110>
- Smyth, H. R., Hall, R., & Nichols, G. J. (2008). Cenozoic volcanic arc history of East Java, Indonesia: The Stratigraphic Record of Eruptions on An Active Continental Margin. In A. E. Draut, P. D. Clift, & D. W. Scholl (Eds.), *Formation and Applications of the Sedimentary Record in Arc Collision Zones* (Vol. 436, pp. 199–222). Geological Society of America. [https://doi.org/10.1130/2008.2436\(10\)](https://doi.org/10.1130/2008.2436(10))
- Smyth, H. R., Crowley, Q. G., Hall, R., Kinny, P. D., Hamilton, P. J., & Schmidt, D. N. (2011). A Toba-scale eruption in the Early Miocene: The Semilir eruption, East Java, Indonesia. *Lithos*, 126(3), 198-211. <https://doi.org/https://doi.org/10.1016/j.lithos.2011.07.010>
- Soeria-Atmadja, R., Maury, R. C., Bellon, H., Pringgoprawiro, H., Polve, M., & Priadi, B. (1994). Tertiary Magmatic Belts in Java. *Journal of Southeast Asian Earth Sciences*, 9(1), 13-27. [https://doi.org/10.1016/0743-9547\(94\)90062-0](https://doi.org/10.1016/0743-9547(94)90062-0)
- Subroto, E. A., Noeradi, D., Priyono, A., Wahono, H. E., Hermanto, E., Praptisih, & Santoso, K. (2007). The Paleogene Basin Within The Kendeng Zone, Central Java Island, and Implications to Hydrocarbon Prospectivity. Indonesian Petroleum Association Thirty-first Annual Convention & Exhibition, Jakarta, Indonesia.
- Surono, Toha, B., & Sudarno, I. (1992). *Peta Geologi Lembar Surakarta - Giritontro, Jawa*. Bandung, Indonesia, Pusat Penelitian dan Pengembangan Geologi.
- Tikhonov, A. N., Goncharsky, A. V., Stepanov, V. V., & Yagola, A. G. (1995). *Numerical Methods for the Solution of Ill-Posed Problems* (1st ed.). Springer-Science+Business Media, B. V. <https://doi.org/10.1007/978-94-015-8480-7>
- UBC-GIF. (2015a, 2017). 6.5. *The Alphas Parameters*. UBC-GIF. Retrieved 19 December from <https://gifttoolscookbook.readthedocs.io/en/latest/content/fundamentals/Alphas.html>
- UBC-GIF. (2015b, 2017). 6.7. *Sparse and Blocky Norms*. UBC-GIF. Retrieved 19 December from <https://gifttoolscookbook.readthedocs.io/en/latest/content/fundamentals/Norms.html>
- Wahyudi, E. J., Santoso, D., & Ahmad Firdaus, M. U. (2019). Gravity Survey in Pandan Mountain - East Java, Indonesia. *Journal of Physics: Conference Series*, 1204, 012006. <https://doi.org/10.1088/1742-6596/1204/1/012006>
- Waltham, D., Hall, R., Smyth, H. R., & Ebinger, C. J. (2008). Basin Formation by Volcanic Arc Loading. In A. E. Draut, P. D. Clift, & D. W. Scholl (Eds.), *Formation and Applications of the Sedimentary Record in Arc Collision Zones* (Vol. 436, pp. 11–26). Geological Society of America. [https://doi.org/10.1130/2008.2436\(02\)](https://doi.org/10.1130/2008.2436(02))